Polyhedron 44 (2012) 221–227

Contents lists available at SciVerse ScienceDirect

Polyhedron

journal homepage: www.elsevier.com/locate/poly

# Synthesis and characterizations of hydride carbonyl ruthenium(II) complexes with (benzimidazol-2-yl)-pyridine ligand

J.G. Małecki *, A. Maroń

*Department of Crystallography, Institute of Chemistry, University of Silesia, ul. Szkolna 9, 40-006 Katowice, Poland*

ARTICLE INFO

*Article history:*
Received 3 June 2012
Accepted 1 July 2012
Available online 9 July 2012

*Keywords:*
Ruthenium hydridocarbonyl complexes
2,6-Bis-(benzimidazol-2-yl)-pyridine
X-ray
Electronic structure
Absorption electronic spectra
DFT
TDDFT

ABSTRACT

The hydride carbonyl ruthenium(II) [RuH(CO)(bzimpy)($PPh_3$)$_2$]Cl·$CH_3OH$ (**1**) and [RuH(CO)(bzimpy)($PPh_3$)$_2$]·$CH_3OH$ (**2**) complexes were synthesized and characterized by IR, $^1H$, $^{31}P$ NMR, UV–Vis spectroscopy and X-ray crystallography. In the complexes the 2,6-bis-(benzimidazol-2-yl)-pyridine functions as bidentate ligand exists as protonated in (**1**) and deprotonated form in (**2**). The experimental studies were complemented by quantum chemical calculations which were used to identify the nature of the interactions between the ligands and the central ion and the orbital compositions in the frontier electronic structures. Based on a molecular orbital scheme, the calculated results allowed the interpretation of the UV–Vis spectra obtained at an experimental level.



## 1. Introduction

Ruthenium(II) complexes with ligands based on pyridine as well as benzimidazole ring are one of the most interesting area of ruthenium coordination chemistry [1–8]. 2,6-Bis-(benzimidazol-2-yl)-pyridine (bzimpy) is an example of combination of these two kinds of ligands and its coordination toward various transition metals is widely studied in many papers and can be characterized as very diverse [9–16]. The special properties of this compound as a ligand is associated with the fact that it contains both pyridine and benzimidazole rings and the differences between coordination behaviors of pyridine and benzimidazole are also responsible for unique nature of bzimpy compared to the ligands including only one type of these heteroaromatic rings such as terpy, bpy. The pyridine ring as a good π–acceptor tends to stabilize the ruthenium(II) acceptor centre better than the imidazole and its derivatives, which exhibit moderate π–donor properties [17].

Although 2,6-bis-(benzimidazol-2-yl)-pyridine is usually described as tridendate ligand, in some cases it can create another possibilities of coordination [9]. Additionally according to some sources the coordination with central atom may increase the ease of dissociation of the benzimidazole NH imino protons [11]. Taking into account these factors, it is not surprising the widespread interest of ruthenium(II) complexes with bzimpy and ligands derived from bzimpy, but up to now it has not been paid too much attention to the hydride carbonyl complexes of ruthenium(II) with this ligand.

Here, we present the synthesis, crystal, molecular and electronic structures, and spectroscopy characterization of two ruthenium(II) hydridocarbonyl complexes with 2,6-bis-(benzimidazol-2-yl)-pyridine ligands. The electronic structures of the complexes have been determined by density functional theory (DFT) and employed for the discussion of bonding properties. The time dependent density functional theory (TD-DFT) was finally used to calculate the electronic absorption spectra. Based on a molecular orbital scheme, the results allowed for the interpretation of the UV–Vis spectra obtained at an experimental level.

## 2. Experimental

All reagents used for the synthesis of the complexes are commercially available and have been used without further purification. The [RuHCl(CO)($PPh_3$)$_3$] complex was synthesized according to the literature method [18].

### 2.1. Synthesis of [RuH(CO)(bzimpy)($PPh_3$)$_2$]Cl·$CH_3OH$ (**1**) and [RuH(CO)(bzimpy)($PPh_3$)$_2$]·$CH_3OH$ (**2**)

The complexes (**1**) and (**2**) were synthesized in a reaction between [RuHCl(CO)($PPh_3$)$_3$] (0.2 g, $2 \times 10^{-4}$ mol) and 2,6-bis-(benzimidazol-2-yl)-pyridine (bzimpy) (0.068 g, $2.2 \times 10^{-4}$ mol) in methanol solutions (100 $cm^3$). In the case of complex (**2**) to the reaction mixture the stoichiometric amount of $NaN_3$ (0.22 mmol)

* Corresponding author.
*E-mail address:* gmalecki@us.edu.pl (J.G. Małecki).

0277-5387/$ - see front matter © 2012 Elsevier Ltd. All rights reserved.
http://dx.doi.org/10.1016/j.poly.2012.07.002

was added. The mixture of the compounds was refluxed in methanol by 4 h. After this time, it was cooled, filtered and left out to slow evaporation.

Complex **1**: Yield. IR (KBr): 3387 $\nu_{OH}$; 3047 $\nu_{ArH}$; 2845 $\nu_{CH}$; 2040 $\nu_{(Ru-H)}$; 1943 $\nu_{(CO)}$; 1603, 1588, 1567 $\nu_{(C=N;\ C=C)}$; 1474 $\delta_{(C-CH\ in\ the\ plane)}$; 1434 $\nu_{Ph(P-Ph)}$; 1092 $\delta_{(C-CH\ in\ the\ plane)}$; 743 $\delta_{(C-C\ out\ of\ the\ plane)}$; 697 $\delta_{(C-C\ in\ the\ plane)}$; 520 $\delta_{(Ru-(H)CO)}$. UV–Vis (methanol; logε): 374 (1.27), 332 (2.46), 260 (sh), 208 (4.75). H NMR (400 MHz, $CDCl_3$) $\delta$: 9.11 (d, $J$ = 79.3 Hz, py), 7.75–6.87 (m, $Ph_{(Im)}$/NH/$PPh_3$), 3.51 (s, $CH_3OH$), −13.19 (t, $J$ = 19.5 Hz, $H_{(Ru)}$).

$^{31}$P NMR (162 MHz, $CDCl_3$) $\delta$: 43.70 (s, $PPh_3$), 42.35 (s, $PPh_3$).

Complex **2**: Yield. IR (KBr): 3393 $\nu_{OH}$; 3046 $\nu_{ArH}$, 1940 $\nu_{(Ru-H/CO)}$; 1600, 1567 $\nu_{(C=N;\ C=C)}$; 1480 $\delta_{(C-CH\ in\ the\ plane)}$; 1434 $\nu_{Ph(P-Ph)}$; 1093 $\delta_{(C-CH\ in\ the\ plane)}$; 737 $\delta_{(C-C\ out\ of\ the\ plane)}$; 694 $\delta_{(C-C\ in\ the\ plane)}$; 519 $\delta_{(Ru-(H)CO)}$. UV–Vis (methanol; logε): 340 (1.26), 291 (2.09), 269 (1.81), 208 (4.92). H NMR (400 MHz, $CDCl_3$) $\delta$: 9.12 (s, py), 8.03–6.85 (m, $Ph_{(Im)}$/NH/$PPh_3$), 3.51 (s, $CH_3OH$), −13.65 (t, $J$ = 19.6 Hz, $H_{(Ru)}$). $^{31}$P NMR ($CDCl_3$) $\delta$: 43.57 (s, $PPh_3$), 42.57 (s, $PPh_3$).

### 2.2. Physical measurements

Infrared spectra were recorded on a Perkin Elmer spectrophotometer in the spectral range 4000–450 $cm^1$ using KBr pellets. Electronic spectra were measured on a Lab Alliance UV–Vis 8500 spectrophotometer in the range of 600–180 nm in methanol solution. The $^1$H and $^{31}$P NMR spectra were obtained at room temperature in $CDCl_3$ using Bruker 400 MHz spectrometer.

### 2.3. Computational methods

The calculations were carried out using Gaussian09 [19] program. Molecular geometries of the singlet ground state of complexes (**1**) and (**2**) were fully optimized in the gas phase at the B3LYP/DZVP level of theory. [20,21] For each compound a frequency calculation was carried out, verifying that the obtained optimized molecular structure corresponds to an energy minimum, thus only positive frequencies were expected. The DZVP basis set [22] with f functions with exponents 1.94722036 and 0.748930908 was used to describe the ruthenium atom and the basis set used for the lighter atoms (C, N, O, P, H) was 6–31G with a set of "d" and "p" polarization functions. The TD-DFT (time dependent density functional theory) method [23] was employed to calculate the electronic absorption spectra of the complexes in the solvent PCM (Polarizable Continuum Model) model. In this work 90 singlet excited states was calculated as vertical transitions for the complexes. A natural bond orbital (NBO) analysis was also made for all the complexes using the NBO 5.0 package [24] included in Gaussian09. Natural bond orbitals are orbitals localized on one or two atomic centers, that describe molecular bonding in a manner similar to a Lewis electron pair structure, and they correspond to an orthonormal set of localized orbitals of maximum occupancy. NBO analysis provides the contribution of atomic orbitals (s, p, d) to the NBO σ and π hybrid orbitals for bonded atom pairs. In this scheme, three NBO hybrid orbitals are defined, bonding orbital (BD), lone pair (LP), and core (CR), which were analyzed on the atoms directly bonded to or presenting some kind of interaction with the ruthenium atom. The contribution of a group (ligands, central ion) to a molecular orbital was calculated using Mulliken population analysis. GaussSum 2.2 [25] was used to calculate group contributions to the molecular orbitals and to prepare the partial density of states (DOS) spectra. The DOS spectra were created by convoluting the molecular orbital information with Gaussian curves of unit height and FWHM (*Full Width at Half Maximum*) of 0.3 eV.

**Table 1**
Crystal data and structure refinement details of $[RuH(CO)(bzimpyH)(PPh_3)_2]Cl{\cdot}CH_3OH$ (**1**), $[RuH(CO)(bzimpy)(PPh_3)_2]{\cdot}CH_3OH$ (**2**) complexes.

| | **1** | **2** |
|---|---|---|
| Empirical formula | $C_{57}H_{48}ClN_5O_2P_2Ru$ | $C_{57}H_{47}N_5O_2P_2Ru$ |
| Formula weight | 1033.46 | 997.01 |
| $T$ (K) | 295.0(2) | 295.0(2) |
| Crystal system | triclinic | triclinic |
| Space group | $P\bar{1}$ | $P\bar{1}$ |
| *Unit cell dimensions* | | |
| $a$ (Å) | 11.2286(5) | 11.2284(4) |
| $b$ (Å) | 12.1197(6) | 11.9902(3) |
| $c$ (Å) | 19.4523(9) | 19.1843(5) |
| $\alpha$ (°) | 74.554(4) | 108.170(2) |
| $\beta$ (°) | 74.374(4) | 104.036(2) |
| $\gamma$ (°) | 86.348(4) | 93.391(2) |
| $V$ (Å$^3$) | 2457.2(2) | 2355.15(12) |
| $Z$ | 2 | 2 |
| Calculated density (Mg/m$^3$) | 1.397 | 1.406 |
| Absorption coefficient (mm$^{-1}$) | 0.487 | 0.451 |
| F(000) | 1064 | 1028 |
| Crystal dimensions (mm) | 0.20 x 0.12 x 0.04 | 0.17 x 0.14 x 0.06 |
| θ range for data collection (°) | 3.38–25.05 | 3.34–25.05 |
| Index ranges | $-13 \le h \le 13$ | $-13 \le h \le 13$ |
| | $-14 \le k \le 14$ | $-14 \le k \le 14$ |
| | $-23 \le l \le 23$ | $-22 \le l \le 22$ |
| Reflections collected | 20130 | 26607 |
| Independent reflections ($R_{int}$) | 8700 (0.0514) | 8328 (0.0366) |
| Data/restraints/parameters | 8700/0/619 | 8328/0/610 |
| Goodness-of-fit on $F^2$ | 1.060 | 1.027 |
| Final $R$ indices [$I > 2s(I)$] | $R_1$ = 0.0521 | $R_1$ = 0.0311 |
| | $wR_2$ = 0.1161 | $wR_2$ = 0.0762 |
| $R$ indices (all data) | $R_1$ = 0.0832 | $R_1$ = 0.0408 |
| | $wR_2$ = 0.1275 | $wR_2$ = 0.0797 |
| Largest difference in peak and hole | 0.79/−0.42 | 0.53/−0.36 |

### 2.4. Crystal structures determination and refinement

The yellow crystals of $[RuH(CO)(bzimpyH)(PPh_3)_2]{\cdot}CH_3OH$ (**1**) and $[RuH(CO)(bzimpy)(PPh_3)_2]{\cdot}CH_3OH$ (**2**) were mounted in turn on an Xcalibur, Atlas, Gemini Ultra Oxford Diffraction automatic diffractometer equipped with a CCD detector, and used for data collection. X-ray intensity data were collected with graphite monochromated Mo $K\alpha$ radiation ($\lambda$ = 0.71073 Å) at temperature 295.0(2) K, with ω scan mode. Ewald sphere reflections were collected up to $2\theta$ = 50.10. The unit cell parameters were determined from least-squares refinement of the setting angles of 12 205 strongest reflections. Details concerning crystal data and refinement are gathered in Table 1. Lorentz, polarization and empirical absorption correction using spherical harmonics implemented in SCALE3 ABSPACK scaling algorithm [26] were applied. The structure was solved by the Patterson method and subsequently completed by the difference Fourier recycling. All the non-hydrogen atoms were refined anisotropically using full-matrix, least-squares technique. The Ru–H hydrogen atoms were found from difference Fourier synthesis after four cycles of anisotropic refinement, and refined as "riding" on the adjacent carbon atom with individual isotropic temperature factor equal 1.2 times the value of equivalent temperature factor of the parent atom. The Olex2 [27] and SHELXS97, SHELXL97 [28] programs were used for all the calculations. Atomic scattering factors were incorporated in the computer programs.

## 3. Results and discussion

### 3.1. Spectroscopic characterization of the complexes

The $^1$H NMR spectra of the complexes are similar and show a set of signals corresponding to the $PPh_3$ and bzimpy ligands given in experimental section. The spectra are complicated due to set of

benzimidazole and triphenylphosphine protons. The triplets at 3.51 ppm indicate methanol, which occurs as solvent in the structures of the complexes. On the $^1$H NMR spectra signals at high field (−13.19 and −13.65 ppm) indicate the presence of the hydride coordinated with the metal. The shifts of the signals are due to the shielding effect of the metal and to the charge of the hydrogen atom. The Ru–H signals are triplets due to coupling with the two *trans* phosphorus atoms ($J_{HP} \sim 20$ Hz). The $^{31}$P NMR spectra of the complexes show two signals at 43.70, 42.35 ppm in complex (**1**) and 43.57, 42.57 ppm on the spectrum of **2**. The presence of magnetically unequivalent phosphorus atoms suggests the presence of two triphenylphosphine groups not in perfect *trans* positions.

The IR spectrum of the cationic complex **1** displays strong C≡O band at 1943 cm$^{-1}$ and the Ru–H stretching bands are displayed at 2040 cm$^{-1}$. On the spectrum of complexes **2** the Ru–CO and Ru–H bands are combined with the maximum of broad band at 1940 cm$^{-1}$. The $\nu_{CO}$ and $\nu_{Ru-H}$ stretching bands in the parent [RuHCl(CO)(PPh$_3$)$_3$] complex are at 1922 and 2020 cm$^{-1}$ respectively and the decreasing of carbonyl stretches are clearly visible in the studied complexes. The decrease in the vibration frequency of the CO bond, compared with starting ruthenium(II) complex, is connected with delivering electron density via backbonding to the anti-bonding orbitals of the CO by benzimidazole in *trans* position to CO. The IR spectrum of complex **1** presents Fig. 1.

### 3.2. Molecular structures

Crystals of the complexes suitable for single crystal X-ray analyses were obtained by slow evaporation of the reaction mixtures. The complexes crystallize in triclinic $P\bar{1}$ space group as solvate with one methanol molecule. Fig. 2 presents their molecular structures and the selected bond distances and angles are collected in Table 2. The bond lengths are similar in both complexes and comparable with distances in other hydride–carbonyl ruthenium(II) complexes with N-heteroaromatic ligands. Knowing about the limits of Fourier synthesis and the problems in recognizing artifacts in the immediate neighborhood of heavy atoms it is doubtful if a reliable position for the hydrogen atom bound to the Ru-atom can be found in the difference Fourier map avoiding the danger of mistaking the effects of the series termination errors for a true atomic position. In the studied complexes the Ru–H distances do not differ significantly from the values for other ruthenium carbonyl hydride complexes found in Cambridge Structural Database (CSD; ConQuest v. 1.14; 2012). The structures of the complexes can be considered as a distorted octahedral with the largest deviation from the expected 90° bond angles coming from the bite angle of 2,6-bis-(benzimidazol-2-yl)-pyridine. It equals to 74.80(12)° and 74.95(6)° for N–Ru–N and 110.01(15)°, 108.35(8)° for C(1)–Ru(1)–N(2) angles in complexes (**1**) and (**2**), respectively. The P–Ru–P angles are lower than 180° vary in the 172.21(4)° to 168.59(2)° range which is confirmed by the presence of two signals at $^{31}$P NMR spectra. As shown in Fig. 2, the CO groups are in the *trans* positions to the benzimidazole ring and the hydride ligands are in *trans* to pyridine ring in the complexes.

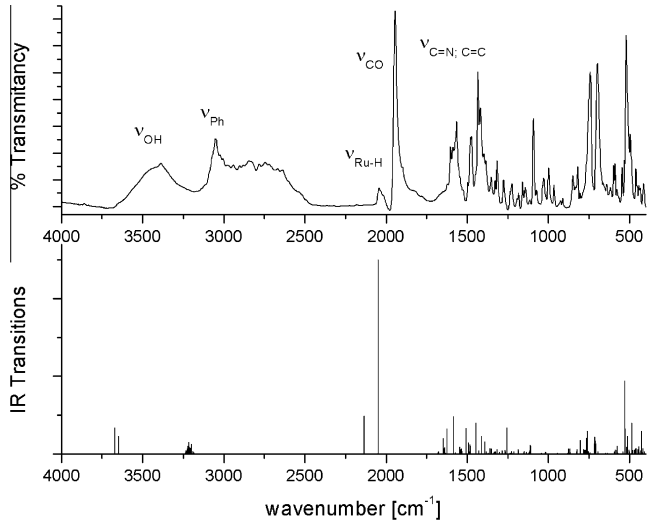


**Fig. 1.** The experimental and calculated IR spectra of [RuH(CO)(MeImCOO)(PPh$_3$)$_2$]·CH$_3$OH complex.

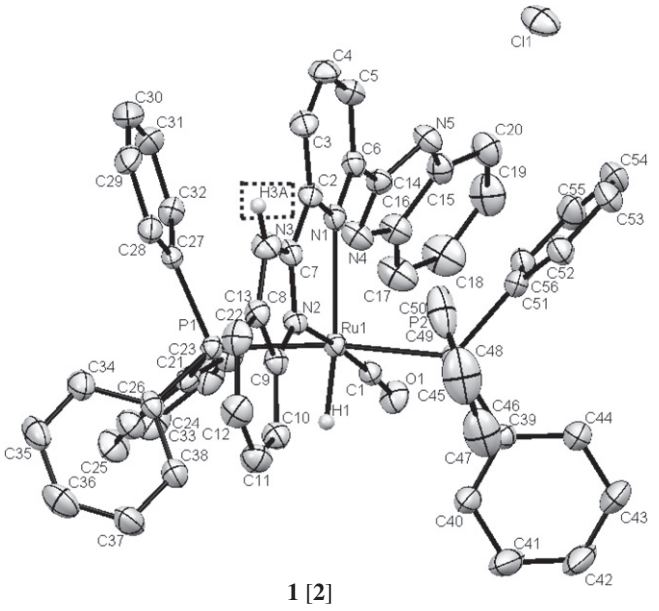


**1** [**2**]

**Fig. 2.** ORTEP drawings of [RuH(CO)(MeImCOO)(PPh$_3$)$_2$]·CH$_3$OH (**1**) and[RuH(CO)(BImCOO)(PPh$_3$)$_2$] (**2**) and complexes with 30% probability displacement ellipsoids. Hydrogen atoms (except Ru–H) and solvent are omitted for clarity.

**Table 2**
Selected bond lengths (Å) and angles (°) of [RuH(CO)(bzimpy)(PPh$_3$)$_2$]Cl·CH$_3$OH (**1**) and [RuH(CO)(bzimpy)(PPh$_3$)$_2$]·CH$_3$OH (**2**) complexes.

| | **1** | | **2** | |
|---|---|---|---|---|
| | Exp | Calc | Exp | Calc |
| *Bond lengths (Å)* | | | | |
| Ru(1)–H(1) | 1.47(4) | 1.58 | 1.49(2) | 1.59 |
| Ru(1)–P(1) | 2.3907(11) | 2.48 | 2.3815(6) | 2.47 |
| Ru(1)–P(2) | 2.3535(11) | 2.45 | 2.3419(6) | 2.43 |
| Ru(1)–N(1) | 2.365(3) | 2.52 | 2.3707(17) | 2.47 |
| Ru(1)–N(2) | 2.106(3) | 2.16 | 2.1114(18) | 2.14 |
| Ru(1)–C(1) | 1.838(4) | 1.88 | 1.841(2) | 1.88 |
| C(1)–O(1) | 1.155(5) | 1.16 | 1.154(3) | 1.16 |
| *Angles (°)* | | | | |
| P(1)–Ru(1)–H(1) | 86.2(17) | 84.7 | 85.6(10) | 84.7 |
| P(2)–Ru(1)–H(1) | 86.5(17) | 84.8 | 83.9(10) | 84.2 |
| P(2)–Ru(1)–P(1) | 172.21(4) | 169.4 | 168.59(2) | 168.7 |
| P(2)–Ru(1)–N(2) | 93.81(8) | 94.2 | 95.84(4) | 94.7 |
| N(1)–Ru(1)–H(1) | 88.8(16) | 90.0 | 92.9(10) | 90.8 |
| N(1)–Ru(1)–P(1) | 86.55(9) | 87.6 | 86.02(5) | 86.6 |
| N(1)–Ru(1)–P(2) | 90.46(9) | 91.5 | 90.23(5) | 91.4 |
| N(1)–Ru(1)–N(2) | 74.80(12) | 72.4 | 74.95(6) | 74.0 |
| N(2)–Ru(1)–H(1) | 163.6(16) | 163.2 | 167.9(10) | 164.8 |
| N(2)–Ru(1)–P(1) | 92.34(8) | 94.2 | 93.59(4) | 95.4 |
| C(1)–Ru(1)–H(1) | 86.4(16) | 85.7 | 83.7(10) | 86.7 |
| C(1)–Ru(1)–P(1) | 93.81(13) | 90.9 | 94.41(7) | 92.5 |
| C(1)–Ru(1)–P(2) | 88.56(13) | 89.3 | 88.71(7) | 89.0 |
| C(1)–Ru(1)–N(1) | 175.14(15) | 176.4 | 176.62(8) | 177.4 |
| C(1)–Ru(1)–N(2) | 110.01(15) | 111.1 | 108.35(8) | 108.5 |
| Ru(1)–C(1)–O(1) | 173.4(4) | 174.9 | 174.17(19) | 174.6 |

In the molecular structures of the complexes several inter- and intra- molecular hydrogen bonds [29] exist what is collected in Table 3. Additionally in the structure of the complexes some electronic interactions (π–π stacking) between $PPh_3$ phenyl and imidazole and pyridine rings from bzimpy are visible and Fig. 3 presents the alignment of centroids formed by imidazole, pyridine and phosphine phenyl rings. The plane-to-plane distances between the phosphine phenyl centroids, determined by C(37) to C(42) and C(45) to C(50) carbons, and imidazole and pyridine rings of bzimpy are equal to 3.80 Å and 3.55 Å with angles between the normal to the centroids of 22.83° and 19.51° (shift distances 1.31 Å and 0.33 Å) in complex **1** indicating π–π stacking interactions. A similar arrangement between aromatic rings occurs in the structure of the complex **2**, where the distances between phenyl rings and imidazole, pyridine centroids are 3.70 Å and 3.63 Å and angles between the normal to the centroids equal to 18.65° and 20.23°. Additionally in the structures of the complexes some intermolecular C–H…π-ring interactions are visible. Fig. 4 presents the interactions between C(4)–H(4)…C(4)[−*x*;−*y*;1 − *z*] and C(36)–H(36)…H(16)[−1 + *x*;*y*;*z*] in the complexes **1** and **2,** respectively. The C–H…π-ring distances are 3.378 Å and 2.843 Å and the electrostatic potentials surfaces presented on Fig. 4 allow these specifying as some stacking interactions.

**Table 3**
Hydrogen bonds for [RuH(CO)(bzimpy)($PPh_3$)$_2$]Cl·$CH_3OH$ (**1**) and [RuH(CO)(bzimpy)($PPh_3$)$_2$]·$CH_3OH$ (**2**) complexes (Å and °).

| D–H···A | d(D–H) | d(H···A) | d(D···A) | <(DHA) |
|---|---|---|---|---|
| **1** | | | | |
| O(2)–H(2)…Cl(1) | 0.82 | 2.27 | 3.076(7) | 168.0 |
| N(3)–H(3A)…Cl(1) #1 | 0.86 | 2.21 | 3.041(4) | 162.1 |
| N(5)–H(5A)…Cl(1) | 0.86 | 2.33 | 3.136(4) | 156.4 |
| C(22)–H(22)…N(4) | 0.93 | 2.40 | 3.324(6) | 170.7 |
| **2** | | | | |
| O(2)–H(2)…N(2) #2 | 0.82 | 1.90 | 2.715(3) | 172.9 |
| N(5)–H(5A)…O(2) #3 | 0.86 | 1.98 | 2.757(3) | 150.0 |
| C(10)–H(10)…N(2) | 0.93 | 2.60 | 2.908(3) | 99.6 |
| C(22)–H(22)…N(4) | 0.93 | 2.37 | 3.296(4) | 179.1 |

Symmetry transformations used to generate equivalent atoms: #1 −*x*, −*y*,1 − *z*; #2 1−*x*,1 − *y*,1 − *z*; #3 1 + *x*,*y*,*z*.

### 3.3. Optimized geometries, hybrid and molecular orbitals description

The ground states geometries of the complexes were optimized in singlet states using the DFT method with the B3LYP functional. The calculations were carried out for gas phase molecules and in general, the predicted bond lengths and angles are in an agreement with the values based on the X-ray crystal structure data, and the general trends observed in the experimental data are reproduced in the calculations (see Table 2). The calculated IR frequencies of complexes **1,** which are shown in Fig. 1, confirm calculated structures with experimental ones and the differences in calculated and experimental spectra mainly result from the negligence of intermolecular interactions for the gas phase. From the data collected in Table 2, one may see that the major of differences between the experimental and calculated geometries are found in the Ru–H and Ru–N(1) distance (∼0.1 Å) and the differences between angles do not exceed 3°.

The NBO analyses, which allowed to know the nature of the coordination between ruthenium and the atoms of the ligands directly interacting with it, were performed for the complexes. This methodology also gave a better understanding of the optimized molecular structures. In the analyses were found that the bzimpy as N,N–donor ligands do not show covalent bonding with ruthenium. The Coulomb-type interactions between the ruthenium central ions and bzimpy ligands are clearly visible in the calculated

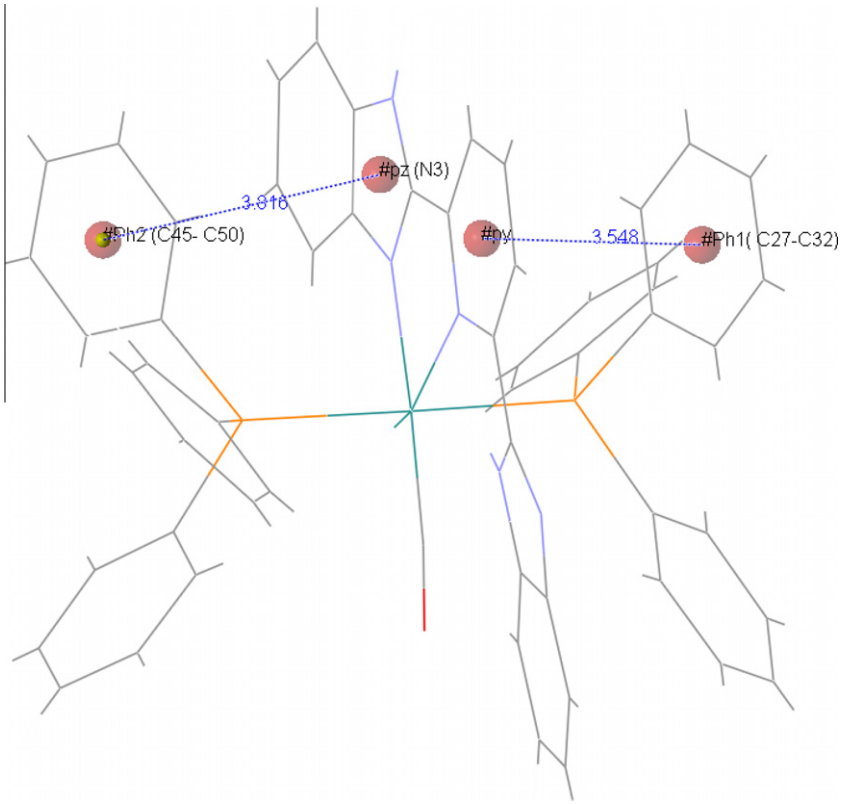


**Fig. 3.** The π-stacking interactions in the molecules of [RuH(CO)(MeImCOO)($PPh_3$)$_2$]·$CH_3OH$ (**1**) and [RuH(CO)(BImCOO)($PPh_3$)$_2$] (**2**) complexes.

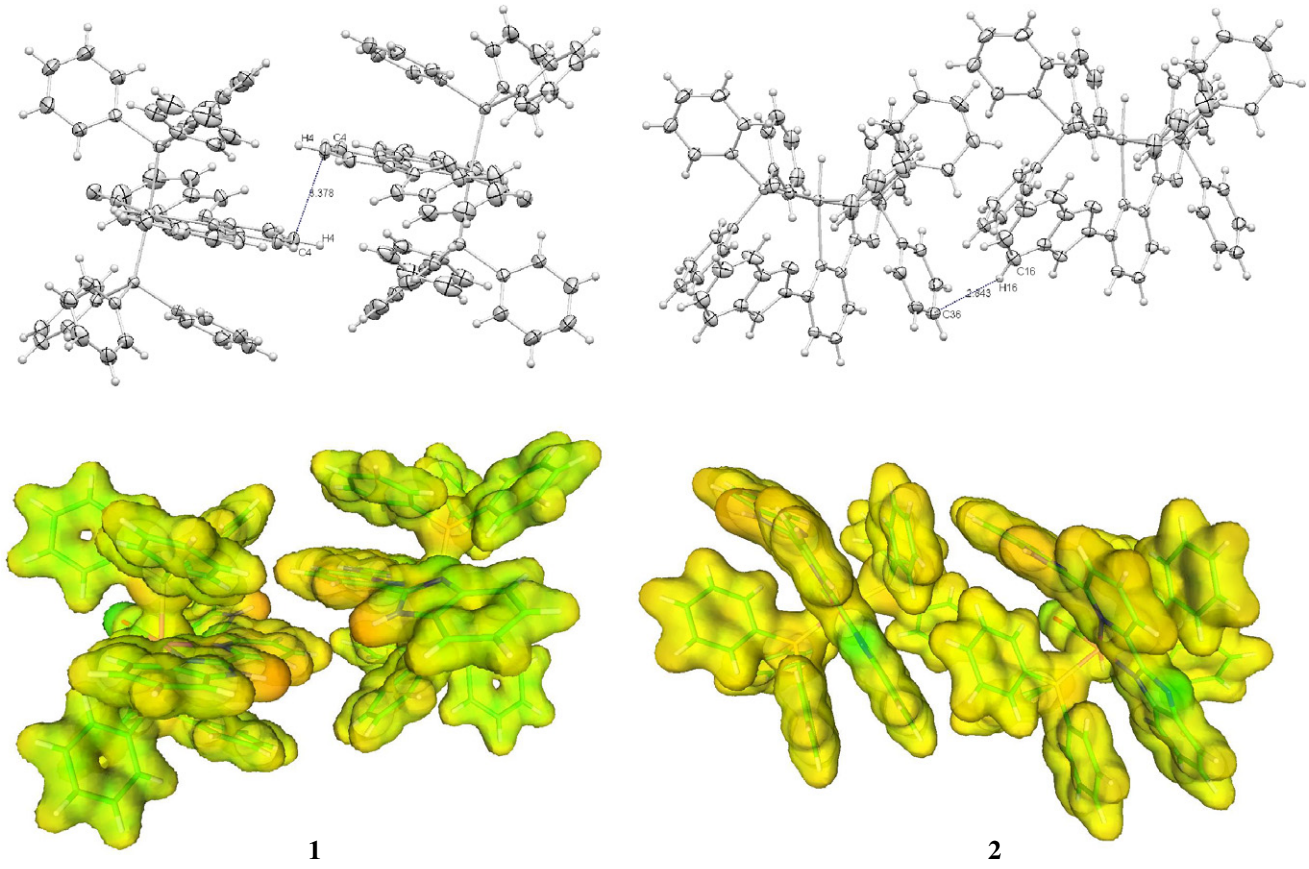


**Fig. 4.** The density of states (DOS) diagrams for the complexes **1** and **2**.

Wiberg bond indices whose values are considerably lower than one. The Ru–$N_{Im}$ and Ru–$N_{py}$ bond indices are similar and close to 0.41, 0.46 and 0.29, 0.32 in the complexes **1** and **2**, respectively. The Ru–P bond orders are also smaller than 1 (∼0.7). For the carbonyl groups of the complexes, three natural bond orbitals were detected for the C–O bond, and one for the Ru–C bond. The Ru–C bond orbitals are polarized towards the carbon atom, and the C–O bond orbitals are polarized towards the oxygen end. The oxygen atom of the carbonyl ligand has one lone pair (LP) orbital. The occupancies and hybridization of the Ru–H, Ru–C and CO bonds are gathered in Table 4 (*anti*-bonding NBOs are given in round brackets). The charge of CO ligands, calculated by summing the individual charges on the carbon and oxygen atoms, have values equal to 0.23 and 0.19 in complexes **1** and **2,** respectively. The values show that there are some charge transfer between CO and the Ru fragment. The Wiberg indexes of the CO bonds in the complexes are reduced (by about 0.20) with respect to free CO ($W_{CO}$ = 2.23). These values are in agreement with the elongation of the C–O bond in complexes and charge distribution in the terminal bonding carbonyl group to ruthenium central ion. The bonding can be described as the result of two electron transfers. First this binding mode involves a σ-donation from the CO lone pair orbital to the LUMO orbital of complex. On the other hand, the highest occupied orbitals of the metallic fragment, mainly $4d_{Ru}$ orbitals, are involved in a π back-bonding from the metal to the CO π* orbitals. The interactions are visible on the overlap density-of-states diagram presented in the Fig. 5. In the frontier HOMOs the bonding interactions between carbonyl and ruthenium(II) central ions appear ($d_{Ru} \rightarrow \pi^*CO$). The σ-donation from CO to $d_{Ru}$ plays role in the higher LUMOs. The ruthenium *d* orbitals occupancies in the complexes are similar and as follow: $d_{xy}$ 1.36, $d_{xz}$ 1.40, $d_{yz}$ 1.63, $d_{x^2-y^2}$ 1.75, $d_{z^2}$ 1.54. The ruthenium(II) central ions natural charges are also similar in the complexes and considerable lower than formal +2 (−0.77). On the Fig. 5 the ruthenium–hydride ion interaction shows strong bonding affect which is in accordance with

**Table 4**
The occupancies and hybridization of the calculated R–H, Ru–C and C≡O natural bond orbitals (NBOs) of [RuH(CO)(bzimpy)($PPh_3$)$_2$]Cl·$CH_3OH$ (**1**) and [RuH(CO)(bzimpy)($PPh_3$)$_2$]·$CH_3OH$ (**2**) complexes.

| BD (2-center bond) | Occupancy | Hybridization of NBO | Wiberg bond indices |
|---|---|---|---|
| | Ru–H | | |
| **1** | 1.852 (0.103) | $0.74(sp^{0.58}d^{2.78})_{Ru} + 0.681(s)_H$ | 0.80 |
| **2** | 1.852 (0.111) | $0.73(sp^{0.64}d^{2.85})_{Ru} + 0.683(s)_H$ | 0.79 |
| | Ru–C | | |
| **1** | 1.942 (0.154) | $0.568(sp^{0.78}d^{2.33})_{Ru} + 0.823(sp^{0.49})_C$ | 1.24 |
| **2** | 1.944 (0.160) | $0.566(sp^{0.84}d^{2.32})_{Ru} + 0.825(sp^{0.48})_C$ | 1.27 |
| | C≡O | | |
| **1** | 1.996 (0.205) | $0.490(sp)_C + 0.872(sp)_O$ | 2.06 |
| | 1.993 (0.168) | $0.508(sp^{15.87})_C + 0.861(p^{10.34})_O$ | |
| | 1.993 (0.045) | $0.544(sp^{2.69})_C + 0.839(sp^{1.60})_O$ | |
| **2** | 1.996 (0.221) | $0.485(sp)_C + 0.875(p)_O$ | 2.03 |
| | 1.994 (0.193) | $0.499(sp^{29.41})_C + 0.866(sp^{18.30})_O$ | |
| | 1.994 (0.032) | $0.548(sp^{2.42})_C + 0.836(sp^{1.36})_O$ | |

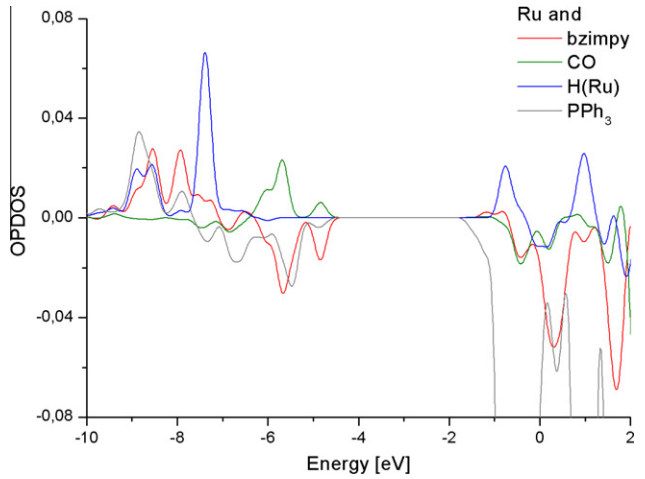


**Fig. 5.** The overlap partial density of states diagrams (OPDOS) for the **1** and **2** complexes.

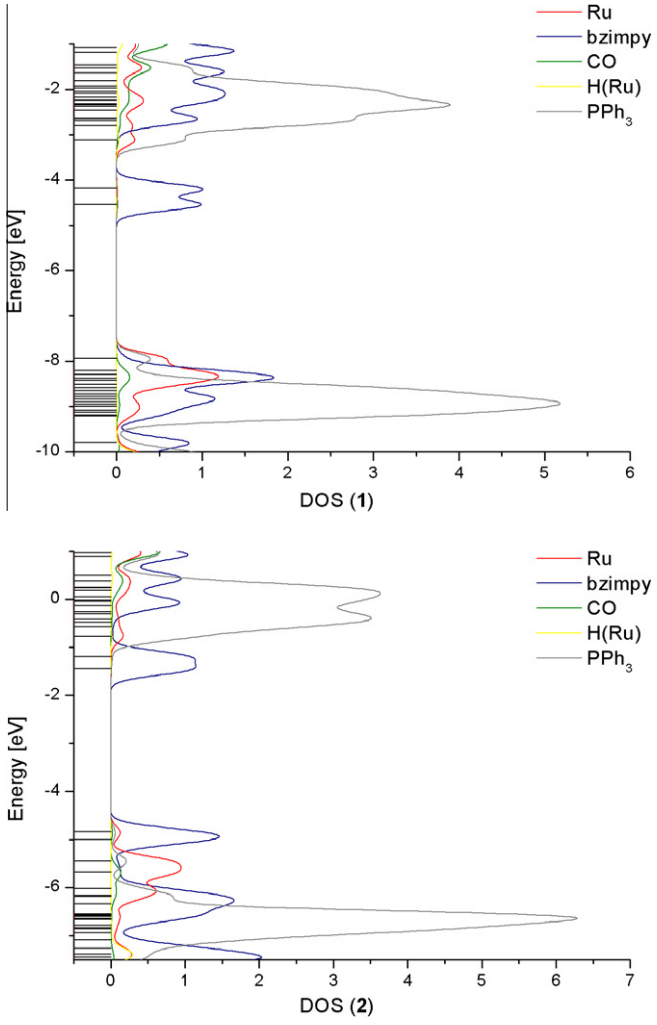


**Fig. 6.** The fluorescence spectra of the **1** and **2** complexes in the dichloromethane solutions ($c = 1 \times 10^{-3}$ mol/dm$^3$).

calculated Wiberg indices (Table 4) showing covalent character of Ru–H bond as well as with the bond distance shorter than 1.5 Å (Table 2). Considering the interaction of bzimpy ligand with ruthenium central ion, one can see that it shows strong acceptor property, which is related to the nature of the aromatic rings in the 2,6-bis-(benzimidazol-2-yl)-pyridine molecule.

**Table 5**
The calculated electronic transitions for $[RuH(CO)(bzimpy)(PPh_3)_2]^+$ (**1**) and $[RuH(CO)(bzimpy)(PPh_3)_2]$ (**2**) complexes.

| (nm) | f | Transitions | Charter |
|---|---|---|---|
| | | **1** | |
| 414.7 | 0.0149 | HOMO → LUMO (90%) | $d_{Ru}/\pi_{bzimpy} \rightarrow \pi_{bzimpy}$ |
| 380.4 | 0.0495 | H-1 → LUMO (77%) | $d_{Ru}/\pi_{bzimpy} \rightarrow \pi_{bzimpy}$ |
| 374.4 | 0.0144 | H-2 → LUMO (65%) | $d_{Ru}/\pi_{bzimpy} \rightarrow \pi_{bzimpy}$ |
| 365.0 | 0.0311 | HOMO → L+1 (94%) | $d_{Ru} \rightarrow \pi_{bzimpy}$ |
| 349.2 | 0.1895 | H-3 → LUMO (55%); H-2 → LUMO (22%) | $d_{Ru}/\pi_{bzimpy} \rightarrow \pi_{bzimpy}$ |
| 334.5 | 0.0274 | H-1 → L+1 (55%) | $d_{Ru}/\pi_{bzimpy} \rightarrow \pi_{bzimpy}$ |
| 332.5 | 0.0217 | H-4 → LUMO (63%); H-3 → LUMO (22%) | $d_{Ru//}\pi_{bzimpy} \rightarrow \pi_{bzimpy}$ |
| 318.3 | 0.3554 | H-6 → LUMO (54%); H-3 → L+1 (30%) | $d_{Ru}/\pi_{PPh3//}\pi_{bzimpy} \rightarrow \pi_{bzimpy}$ |
| 263.6 | 0.0763 | HOMO → L+6 (60%) | $d_{Ru}/\pi_{bzimpy} \rightarrow \pi_{PPh3/bzimpy}$ |
| 262.5 | 0.2066 | H-5 → L+2 (41%); HOMO → L+6 (15%) | $d_{Ru}/\pi_{PPh3} \rightarrow d/\pi_{bzimpy}$ |
| | | **2** | |
| 390.5 | 0.0216 | HOMO → LUMO (95%) | $d_{Ru}/\pi_{bzimpy} \rightarrow \pi_{bzimpy}$ |
| 372.0 | 0.1480 | H-1 → LUMO (80%) | $\pi_{bzimpy} \rightarrow \pi_{bzimpy}$ |
| 364.3 | 0.0481 | HOMO → L+1 (89%) | $d_{Ru}/\pi_{bzimpy} \rightarrow \pi_{bzimpy}$ |
| 358.6 | 0.0291 | H-2 → LUMO (63%) | $d_{Ru} \rightarrow \pi_{bzimpy}$ |
| 355.5 | 0.1068 | H-2 → LUMO (11%); H-2 → L+2 (39%); HOMO → L+2 (24%) | $d_{Ru}/\pi_{bzimpy} \rightarrow \pi_{bzimpy/PPh3}$ |
| 341.3 | 0.2679 | H-3 → LUMO (12%); H-2 → LUMO (12%); H-2 → L+1 (21%) | $d_{Ru}/\pi_{bzimpy/CO} \rightarrow \pi_{bzimpy}$ |
| 336.1 | 0.0105 | H-3 → LUMO (65%); H-2 → L+1 (24%) | $d_{Ru}/\pi_{bzimpy/CO} \rightarrow \pi_{bzimpy}$ |
| 297.2 | 0.0997 | H-4 → LUMO (77%) | $d_{Ru}/\pi_{bzimpy/CO} \rightarrow \pi_{bzimpy}$ |
| 292.3 | 0.0361 | H-5 → LUMO (86%) | $\pi_{bzimpy/PPh3} \rightarrow \pi_{bzimpy}$ |
| 284.9 | 0.152 | H-4 → L+1 (67%) | $d_{Ru}/\pi_{bzimpy/CO} \rightarrow \pi_{bzimpy}$ |
| 267.6 | 0.0103 | H-2 → L+6 (82%) | $d_{Ru} \rightarrow \pi_{bzimpy}$ |
| 264.8 | 0.0231 | HOMO → L+10 (38%); HOMO → L+11 (21%) | $d_{Ru}/\pi_{bzimpy} \rightarrow \pi_{PPh3}$ |

Analysis of the frontier molecular orbitals is useful for understanding the spectroscopic properties such as electronic absorption and emission spectra of organometallic complexes. The electronic structure of complexes **1** and **2** are similar because of similar composition of their coordination sphere. The densities of states (DOS) in terms of Mulliken population analysis were calculated using the GaussSum program and Fig. 6 presents the composition of the fragment orbitals contributing to the molecular orbitals for complexes **1** and **2**. The HOMOs are mainly localized on the ruthenium atoms with contribution from bzimpy ligand. The participations of $d_{Ru}$ orbitals in HOMO to HOMO–5 in the electronic structures of the complexes are in the range from 74% to 35%. The $d_z^2$ ruthenium orbital plays role in LUMO+2 and $d_{x^2-y^2}$ orbitals participate in LUMO+12 in the complexes. LUMO and LUMO+1 are localized on the bzimpy ligands.

### 3.4. Experimental and theoretical electronic spectra

The UV–Vis spectra of the complexes **1** and **2** are similar and the maxima close to 374, 332, 260 nm and 340, 291, 269 nm were measured. Based on the calculated electronic structure of the complexes the bzimpy ligands participations in the transitions are expected. The electronic spectra of the complexes were calculated with the TDDFT method with methanol as solvent in the Polarizable Continuum Model (PCM). As one can see from the data collected in Table 5 the *Charge Transfer* transitions are dominant in the electronic spectra of the complexes. These calculated transitions up to ~260 nm have *Metal-to-Ligand Charge Transfer* charac-

ter with a significant share of π-orbitals of bzimpy ligand. The transitions proceed between the frontier HOMOs and LUMOs (mainly LUMO+1/+2). Due to the localization of LUMO, LUMO+1/+2 on the bzimpy and share of this ligand in HOMOs involved in the transitions, the *Ligand-to-Ligand Charge Transfer* character plays role in the UV–Vis spectrum of the complexes.

Summarizing two new ruthenium(II) complexes with 2,6-bis-(benzimidazol-2-yl)-pyridine functions as bidentate ligand were synthesized and characterized by infra red, proton and phosphorus nuclear magnetic resonance, electronic absorption spectroscopy and X-ray crystallography. In the complexes the bzimpy ligand exists as protonated in $[RuH(CO)(bzimpy)(PPh_3)_2]Cl{\cdot}CH_3OH$ complex and deprotonated form in $[RuH(CO)(bzimpy)(PPh_3)_2]{\cdot}CH_3OH$ obtained in the reaction in the presence of azide anion. In the crystal structure of the complexes, some types of noncovalent interactions between aromatic rings have been found. Electronic structures of the complexes have been determined using the density functional theory (DFT) method, and employed for discussion of its properties. The bzimpy ligands play significant role in their electronic structure and have a dominant participation in the UV–Vis spectra. The lack of luminescence of these complexes is probably related with the mixed nature of the transitions in which the MLCT transitions have significant share of the LLCT character.

## Acknowledgement

Calculations have been carried out in Wroclaw Centre for Networking and Supercomputing (http://www.wcss.wroc.pl).

## Appendix A. Supplementary data

CCDC 871977 and 871976 contains the supplementary crystallographic data for $[RuH(CO)(bzimpy)(PPh_3)_2]Cl{\cdot}CH_3OH$ and $[RuH(CO)(bzimpy)(PPh_3)_2]{\cdot}CH_3OH$ complexes. These data can be obtained free of charge via http://www.ccdc.cam.ac.uk/conts/retrieving.html, or from the Cambridge Crystallographic Data Centre, 12 Union Road, Cambridge CB2 1EZ, UK; fax: (+44) 1223-336-033; or e-mail: deposit@ccdc.cam.ac.uk.

## References

[1] T.-J.J. Kinnunen, M. Haukka, E. Pesonen, T.A. Pakkanen, J. Organomet. Chem. 655 (2002) 31.
[2] C.G. Hotze, J.G. Haasnoot, J. Reedijk, J. Inorg. Biochem. 96 (2003) 152.
[3] Y. Nakabayashi, Y. Hirosaki, O. Yamauchi, Bioelectrochemistry 69 (2006) 216.
[4] A. Batista, M.O. Santiago, C.L. Donnici, I.S. Moreira, P.C. Healy, S.J. Berners-Price, S.L. Queiroz, Polyhedron 20 (2001) 2123.
[5] Xiang-Yong Lu, Hui-Jun Xu, Xue-Tai Chen, Inorg. Chem. Commun. 12 (2009) 887.
[6] Amardeep Singh, Gopal Das, Biplab Mondal, Polyhedron 27 (2008) 2563.
[7] Huai-Xia Yang, Yan-Ju Liu, Lin Zhao, Ke-Zhi Wang, Spectrochimica Acta A. 76 (2010) 146.
[8] N. Bharti, M.R. Maurya, F. Naqvi, A. Azam, Bioorg. Med. Chem. Lett. 10 (2000) 2243.
[9] M. Boča, R.F. Jameson, W. Linert, Coord. Chem. Rev. 255 (2011) 290.
[10] W. Linert, M. Konecny, F. Renz, J. Chem. Soc., Dalton Trans. (1994) 1523.
[11] X. Xiaoming, M. Haga, T. Matsumura-Inoue, Y. Ru, A.W. Addison, K. Kano, J. Chem. Soc., Dalton Trans. (1993) 2477.
[12] E. Ceniceros-Gómez, A. Ramos-Organillo, J. Hernández-Díaz, J. Nieto-Martínez, R. Contreras, S.E. Castillo-Blum, Heteroat. Chem. 11 (2000) 392.
[13] W. Addison, S. Burman, C.G. Wahlgren, O.A. Rajan, T.M. Rowe, E. Sinn, J. Chem. Soc., Dalton Trans. (1987) 2621.
[14] S. Chit Yu, S. Hou, W. Kin Chan, Macromolecules 32 (1999) 5251.
[15] D. Mishra, S. Naskar, S.K. Chattopadhyay, M. Maji, P. Sengupta, R. Dinda, S. Ghosh, T.C.W. Mak, Transit. Met. Chem. 30 (2005) 352.
[16] M. Haga, H.-G. Hong, Y. Shiozawa, Y. Kawata, H. Monjushiro, T. Fukuo, R. Arakawa, Inorg. Chem. 39 (2000) 4566.
[17] P. Sengupta, R. Dinda, S. Ghosh, Polyhedron 20 (2001) 3349.
[18] N. Ahmad, J.J. Levinson, S.D. Robinson, M.F. Uttely, Inorg. Synth. 15 (1974) 48.
[19] M.J. Frisch, G.W. Trucks, H.B. Schlegel, G.E. Scuseria, M.A. Robb, J.R. Cheeseman, G. Scalmani, V. Barone, B. Mennucci, G.A. Petersson, H. Nakatsuji, M. Caricato, X. Li, H.P. Hratchian, A.F. Izmaylov, J. Bloino, G. Zheng, J.L. Sonnenberg, M. Hada, M. Ehara, K. Toyota, R. Fukuda, J. Hasegawa, M. Ishida, T. Nakajima, Y. Honda, O. Kitao, H. Nakai, T. Vreven, J.A. Montgomery Jr., J.E. Peralta, F. Ogliaro, M. Bearpark, J.J. Heyd, E. Brothers, K.N. Kudin, V.N. Staroverov, R. Kobayashi, J. Normand, K. Raghavachari, A. Rendell, J.C. Burant, S.S. Iyengar, J. Tomasi, M. Cossi, N. Rega, J.M. Millam, M. Klene, J.E. Knox, J.B. Cross, V. Bakken, C. Adamo, J. Jaramillo, R. Gomperts, R.E. Stratmann, O. Yazyev, A.J. Austin, R. Cammi, C. Pomelli, J.W. Ochterski, R.L. Martin, K. Morokuma, V.G. Zakrzewski, G.A. Voth, P. Salvador, J.J. Dannenberg, S. Dapprich, A.D. Daniels, O. Farkas, J.B. Foresman, J.V. Ortiz, J. Cioslowski, D.J. Fox, Gaussian 09, Revision A.1, Gaussian Inc., Wallingford, CT, 2009.
[20] A.D. Becke, J. Chem. Phys. 98 (1993) 5648.
[21] C. Lee, W. Yang, R.G. Parr, Phys. Rev. B 37 (1988) 785.
[22] K. Eichkorn, F. Weigend, O. Treutler, R. Ahlrichs, *Theor. Chim. Acc.* 97 (1997) 119.
[23] M.E. Casida, in: J.M. Seminario (Ed.), Recent Developments and Applications of Modern Density Functional Theory, Theoretical and Computational Chemistry, vol. 4, Elsevier, Amsterdam, 1996, p. 391.
[24] NBO Version 3.1, E. D. Glendening, A. E. Reed, J. E. Carpenter, and F. Weinhold.
[25] N.M. O'Boyle, A.L. Tenderholt, K.M. Langner, J. Comp. Chem. 29 (2008) 839.
[26] CrysAlis RED, Oxford Diffraction Ltd., Version 1.171.29.2.
[27] O.V. Dolomanov, L.J. Bourhis, R.J. Gildea, J.A.K. Howard, H. Puschmann, J. Appl. Crystallogr. 42 (2009) 339.
[28] G.M. Sheldrick, Acta Cryst. A64 (2008) 112.
[29] G.R. Desiraju, T. Steiner, The Weak Hydrogen Bond in Structural Chemistry and Biology, Oxford University Press, 1999.